Universal features and tail analysis of the order-parameter distribution of the two-dimensional Ising model: An entropic sampling Monte Carlo study

Anastasios Malakis* and Nikolaos G. Fytas
Department of Physics, Section of Solid State Physics, University of Athens, Panepistimiopolis, GR 15784 Zografos, Athens, Greece
(Received 16 December 2005; published 17 May 2006)

We present a numerical study of the order-parameter probability density function (PDF) of the square Ising model for lattices with linear sizes $L=80-140$. A recent efficient entropic sampling scheme, combining the Wang-Landau and broad histogram methods and based on the high levels of the Wang-Landau process in dominant energy subspaces is employed. We find that for large lattices there exists a stable window of the scaled order-parameter in which the full ansatz including the pre-exponential factor for the tail regime of the universal PDF is well obeyed. This window is used to estimate the equation of state exponent and to observe the behavior of the universal constants implicit in the functional form of the universal PDF. The probability densities are used to estimate the universal Privman-Fisher coefficient and to investigate whether one could obtain reliable estimates of the universal constants controlling the asymptotic behavior of the tail regime.

DOI: 10.1103/PhysRevE.73.056114 PACS number(s): 05.50.+q, 75.10.Hk, 05.10.Ln, 64.60.Fr

I. INTRODUCTION

A significant achievement in the theory of equilibrium critical phenomena was the confirmation of universality and scaling hypotheses and the calculation of critical exponents [1–6]. The finite-size scaling technique has proven to be an extremely reliable and powerful method for determining the critical properties of low-dimensional systems, and several review articles have appeared covering the original finite-size scaling theory and later advancements [7–10]. In practice all universality claims have been put to several tests using data obtained from numerical simulations of finite systems and the extraction of universal behavior from such studies remains today of vigorous research interest. Of particular interest is the view that, a strong hallmark of a universality class may be obtained via the probability density functions of the main thermodynamic variables of the system at criticality [11]. In finite systems the order-parameter may be characterized by a probability distribution function (PDF) and this distribution may be scaled appropriately to provide a sequence of densities that appears to converge rapidly to a unique scaling PDF [12–14]. We may think of this limiting scaling function as the key ingredient specific to a universality class, like the critical exponents [15]. This idea has been elaborated in recent years by many authors, several papers are devoted to the estimation of such universal distributions, and the subject is of great and growing interest [11–13,15–23].

Most properties of finite-size scaling functions are known from numerical simulation of critical systems [12–24]. Analytical results originate from field theoretic renormalization group calculations [25–27], conformal field theory [1,28], but also from a generalized classification theory of phase transitions [29–32]. In a few cases some of the analytical predictions seem to have been confirmed by numerical simulations [19,32]. A detailed investigation of the tail regime was carried out in one of the early multicanonical Monte Carlo simulations by Smith and Bruce [20] for the two-dimensional Ising model, using square lattices of size $L=32$ and $L=64$. Even though these authors managed to measure extremely small tail probabilities with high accuracy, and found signs for the far tail regime conjecture, the theme was not fully elucidated. It is well known that the process of recording the very small probabilities in the tails of the distribution requires specialized numerical techniques and sufficient statistical accumulation is necessary in order to probe the tails confidently.

Some studies using traditional Monte Carlo simulations have attempted to estimate the universal density over the last years, but failed in establishing the true behavior at the far tail regime of the critical order-parameter distribution. Traditional Monte Carlo sampling methods have increased dramatically our understanding of the behavior of the standard classical statistical mechanics systems. The Metropolis method and its variants were, for many years, the main tools in condensed matter physics, particularly for the study of critical phenomena [33–37]. However, this standard approach has certain crucial weaknesses. Importance sampling is trapped for very long times in valleys of rough free energy landscape, as in complex systems in which effective potentials have a complicated rugged landscape. For large systems these trapping effects become more pronounced and the Metropolis method, but also its variants, become inefficient. Moreover, importance sampling methods are unsuccessful in recording of the very small probabilities in the tails of the critical order-parameter distribution. As was pointed out by Hilfer *et al.* [21] the study of the tail regime requires special numerical techniques [19,20,38].

Several new efficient methods that directly calculate the density of states (DOS) of classical statistical models play a dominant role in overcoming the above-mentioned problems in recent years. A few remarkable examples of such methods are the entropic [36,39], multicanonical [40], broad histogram (BH) [41], transition matrix [42] and Wang-Landau

*Author to whom correspondence should be addressed. Electronic address: amalakis@phys.uoa.gr

(WL) [43] methods. It is now possible to study more effectively the finite-size scaling properties of statistical models by using entropic Monte Carlo techniques. The multicanonical Monte Carlo method has already been applied for the evaluation of the tail regime of the universal PDF of the order-parameter [21] and the present paper follows these attempts by using a new simple and efficient entropic technique. This technique will be referred to as the critical minimum energy subspace CrMES-WL entropic sampling scheme [44] and is in fact a program for the simultaneous estimation of all thermal and magnetic finite-size anomalies of the statistical system. The method was recently presented and successfully tested on the square Ising model [44]. The central idea is to optimize the simulations by using in a systematic way only the dominant energy subspaces appropriate to the finite system at the temperature range of interest. As shown in Ref. [44] this restriction speeds up our simulations, but also gives a new route for critical exponent estimation by studying the finite-size scaling of the extensions of the dominant subspaces. This scheme is expected to be much more efficient than the Metropolis algorithm, as already pointed out in a comparative study [44], illustrating its superiority in the recordings of the far tail regime. Overall, the aim of this contribution is twofold: firstly to show that the CrMES scheme is sufficient for the study of the tail regime and therefore to propose a sensible optimization route. Secondly, to yield new evidence confirming the tail regime conjecture and to provide an early estimation of the universal parameters involved.

The rest of the paper is organized as follows: In the next section, we briefly review the CrMES-WL entropic scheme, including the N-fold way implementation of this scheme. This approach is more efficient and makes available an additional approximation for the DOS, based on the BH method. In Sec. III we study the order-parameter distribution of the square Ising model and we verify its asymptotic behavior in the far tail regime. The relevance of our findings to the universal Privman-Fisher coefficient is also discussed and used to observe the self-consistency of our estimations. Our conclusions are summarized in Sec. IV.

II. ENTROPIC SAMPLING IN DOMINANT ENERGY SUBSPACES

Let us briefly describe the Monte Carlo approach implemented in order to generate the numerical data used in the next section. Since the main ingredient of this approach, decisive for its efficiency, is the restriction of the energy spectrum called CrMES restriction, we shall also explain, although briefly, some key ideas about its implementation. For a full description, alternative definitions and further technical details of the CrMES scheme one should consult the original papers, where the method has been recently tested [44–46]. The main idea is to produce accurate estimates for all finite-size thermal and magnetic anomalies of a statistical system by using a DOS method, based on WL random walks, in an appropriately restricted energy subspace (E_1,E_2). In particular it was shown [44] that it is quite accurate to implement this restricted scheme and at the same time accumulate data for the two-parameter energy, magnetization (E,M) histograms, using for their recording only the high-levels of the WL diffusion process. At the end of the process the final accurate WL or the accumulated BH approximation of the DOS and the cumulative (E,M) histograms, are used to determine all properties of the statistical system. This approximation is accurate in a wide temperature range, depending on the extension of the dominant energy subspace used, around the critical temperature of the system and this range can be chosen in such a way that includes all pseudocritical temperatures of the finite system.

A multirange WL algorithm [43] is implemented to obtain the DOS and the (E,M) histograms in the energy subspace (E_1,E_2). The WL modification factor (f_j) is reduced at the jth iteration according to: $f_1=e$, $f_j \rightarrow f_{j-1}^{1/2}$, $j=2,\ldots,J_{\mathrm{fin}}$. The density of states obtained throughout the WL iteration process may be denoted by $G_{\mathrm{WL}}(E)$. This density and the high-level ($j>12$, see also the discussion below) WL (E,M) histograms [denoted by $H_{\mathrm{WL}}(E,M)$] are used to estimate the magnetic properties in a temperature range, which is covered, by the restricted energy subspace (E_1,E_2). The N-fold version of the WL algorithm [47,48] makes available an additional approximation for the DOS [denoted by $G_{\mathrm{BH}}(E)$], based on the BH method. We shall use only the approximation of $G_{\mathrm{BH}}(E)$ corresponding to the minimum energy transitions ($\Delta E=4$) in the N-fold process. $G_{\mathrm{BH}}(E)$ is obtained from the well-known BH equation [41]: $G(E)\langle N(E,E+\Delta E)\rangle_E = G(E+\Delta E)\langle N(E+\Delta E,E)\rangle_{E+\Delta E}$, where $N(E,E+\Delta E)$ is the number of possible spin flip moves from a microstate of energy E to a microstate with energy $E+\Delta E$. The microcanonical average of these numbers is estimated at the end of the CrMES-WL entropic scheme, with the help of the corresponding appropriate histograms recorded in the same high-level WL iteration range, used also for the recording of the (E,M) histograms.

The probability density of the order-parameter at some temperature of interest T may be expressed as follows: [44]

$$P_T(M) \cong \frac{\sum_{E\in(E_1,E_2)} [H_{\mathrm{WL}}(E,M)/H_{\mathrm{WL}}(E)] G_{\mathrm{WL}}(E) e^{-\beta E}}{\sum_{E\in(E_1,E_2)} G_{\mathrm{WL}}(E) e^{-\beta E}}, \tag{1a}$$

where

$$H_{\mathrm{WL}}(E) = \sum_M H_{\mathrm{WL}}(E,M) \tag{1b}$$

and the summation in M runs over all values generated in the restricted energy subspace (E_1,E_2). Since the detailed balance condition depends on the control parameter f_j, it is suggested [44] that only the high-level recipes or their N-fold versions should be used for recording the (E,M) histograms. This practice yields excellent estimates for all magnetic properties as has been shown in detail in Ref. [44].

The performance limitations of entropic methods, such as the WL random walk and the reduction of their statistical fluctuations have recently attracted considerable interest

[51–53]. For the CrMES entropic scheme, presented here in Eq. (1), an extensive comparative study using various implementations was presented in Ref. [44]. In particular, this study has clarified the effect of the used range of the WL iteration levels on the magnetic properties of the system and also the effect of one of the simplest refinements of the WL algorithm. Statistical fluctuations are reduced, as usually, by multiple measurements but also by using the separation refinement proposed by Zhou and Bhatt [52], in which the WL DOS modification is applied after a number $\mathcal{S}$ ($\mathcal{S}=16$) spin-flips. For the recordings of the (E,M) histograms, the range $j=12-24$, of the WL iteration levels, was shown to give accurate estimates for moderate lattice sizes ($L=10-120$), while a range of the order $j=18-28$ would be a more safe choice for larger lattices. Furthermore, as it has been shown recently [44,52,53], the histogram flatness criterion of the WL scheme for reducing the modification factor should be treated with caution, and in order to avoid strong statistical fluctuations in the final approximate DOS, enough statistics should be obtained in each WL iteration.

Let us provide here some further technical details on the implementation of our entropic scheme. For a large system, we divide the total CrMES in several energy ranges of the order of 50–60 energy levels each, overlapping at their ends in at least 3 energy levels. When combining these energy intervals, simple averaging is applied on the entropies of two neighboring pieces at their overlapping end. Then, the DOS for each piece is adjusted to the DOS of its previous neighbor and continuing this procedure we finally obtain the DOS in the total CrMES. We follow a mixed WL process in which in the first stage ($j=1-11$ or $j=1-17$) we use the WL algorithm and in the second stage ($j=12-24$ or $j=18-28$) its N-fold version. This mixed process was also used in a previous study [48], where a generalization of the N-fold version was presented. In the present application only the original Schulz *et al.* [47] N-fold version has been used (case $c=1$ in Ref. [48]). The accumulation of the microcanonical estimators, necessary for the application of the BH equation [41], takes place only in the N-fold stage of the process. At these high levels of the WL random walk, the incomplete detailed balanced condition has not a significant effect on the BH microcanonical estimators and the particular multirange approach seems to be optimal in both time and accuracy requirements. Besides the worse time requirements, our tests indicated also more significant effects (presumably coming from incomplete detailed balanced condition) for a multirange approach using much larger energy intervals. Furthermore, an accurate run requires enough statistics to be obtained during each step of the process.

The resulting WL and BH DOS approximations were tested using our accurate finite-size data for the critical specific heat and the asymptotic formulas discussed in Refs. [45,50]. Using several independent random walks, we have verified that both the final WL and BH estimates for the critical specific heats $[C(T_c)]$ are very accurate, with errors of less than 1%, even for large lattices of the order of $L=200$. In many cases, the BH estimates showed smaller statistical fluctuations when different runs were compared. However, in cases in which insufficient simulations were performed for large lattices ($L=140-200$), a significant underestimation was observed for $C(T_c)$ and this distortion was then much stronger for the BH estimates. A further interesting test, substantiating the statistical reliability of our approach, was performed for the lattice $L=50$ by using the exact DOS obtained by the algorithm provided by Beale [54]. In this test, we applied a one-range exact entropic N-fold sampling to obtain an approximate BH DOS and this was then used to obtain an estimate $C(T_c)$. When this one-range exact entropic estimate of $C(T_c)$ was compared with the corresponding estimate obtained by our multirange and approximate entropic scheme, we found excellent coincidence and in effect the same order of relative errors (0.001–0.0001) compared to the exact result. Similarly, such small relative deviations, between the exact and the approximate entropic schemes, were also observed in the corresponding magnetic properties (for instance for $\sqrt{\langle m^2\rangle}$) and in fact these deviations were less significant than the fluctuations coming from limited magnetic sampling, as observed in different runs. Therefore, we suggest that the unified multi-range implementation of the Wang-Landau [43] algorithm and the BH method of Oliveira *et al.* [41] may be advantageous in studies using entropic schemes.

In the original paper [45], the CrMES method was presented by restricting the energy spectrum around the value $\tilde{E}$, producing the maximum term in the partition function at some temperature of interest. The restriction was imposed by requesting a specified relative accuracy (r) on the value of the specific heat. In other words, the restriction of the energy spectrum produces an error on the value of the thermodynamic parameter, at the particular temperature, and r measures the produced relative error. This relative error is set equal to a small number ($r=10^{-6}$), which is, in any case, much smaller than the statistical errors of the Monte Carlo method (the DOS method) used for the determination of the thermodynamic parameter (for instance the specific heat). It was also shown that a systematic study of the finite-size extensions of the resulting dominant subspaces produces the thermal exponent α/ν with very good accuracy [45]. As pointed out above, this idea may be simultaneously applied [44] for all finite-size anomalies including the magnetic anomalies determined from the (E,M) histograms. Furthermore, very good estimates of the critical exponent γ/ν have been obtained [44] by studying the finite-size extensions of analogous critical minimum magnetic subspaces (CrMMS) defined also below. In this case, the restriction on the order-parameter space around the value $\tilde{M}$ that maximizes the order-parameter density at the critical temperature T_c is imposed on the probability density function, as shown in Eq. (2). That is, the location of the dominant magnetic subspaces $(\tilde{M}_-,\tilde{M}_+)$ may be obtained by comparing the end-point densities with the peak-height of the distribution

$$\tilde{M}_{\pm}:\ \frac{P_{T_c}(\tilde{M}_{\pm})}{P_{T_c}(\tilde{M})} \leqslant r \tag{2}$$

and the critical exponent γ/ν may be estimated from the following scaling law ($\Delta\tilde{M}=(\tilde{M}_+-\tilde{M}_-)$) [44]

$$\frac{(\Delta\tilde{M})^2_{T_c}}{L^d} \approx L^{\gamma/\nu}. \tag{3}$$

One should note here that, the finite-size extensions of the above defined CrMMS can be calculated by any Monte Carlo method producing the order-parameter distribution. One could as well implement the Metropolis algorithm to find estimates of the extensions involved in Eq. (3). However, this will yield a marked underestimation of γ/ν as a result of the statistical insufficiency of this traditional algorithm in the tail regime. This effect was shown to be a result of the very slow equilibration process of the algorithm in the far tail regime of the order-parameter distribution [44]. On the other hand, the CrMES-WL entropic scheme was shown to produce very good estimates of the critical exponent γ/ν [44] and this can be taken as an indication in favor of the suitability of this method in studies of the universal distributions and in particular for their tail regime.

Let us now address the question of adequacy of the CrMES restriction to deal with the far tail regime of the order parameter PDF. In previous Monte Carlo studies [20,21] extensive simulations were undertaken in order to reach, as close as possible, the saturation regime ($M/N \simeq 1$, $N=L^2$) of the order-parameter. This practice is related to the fact that the part of the order-parameter spectrum determining the tail regime is not formally known. Scaling the PDF introduces a variable $x=m/\sqrt{\langle m^2\rangle}$ and the (right) tail regime is expected to be detected in the range $x>1$ [13,20]. Consequently, a main question concerns the sufficiency of the CrMES scheme. Does such a restriction on the energy space yield a reliable approximation in the tail regime? In particular, we would like to know whether this restriction would allow us to simulate the order-parameter in the appropriate range to confirm the tail regime conjecture. The following observations provide strong evidence to this important question and our findings in the next section establish explicitly the fact that the implementation of a CrMES restriction permits an asymptotic evaluation of properties related to the tail regime.

In Fig. 1 we illustrate the effect of various restrictions on the universal PDF (for details see next section) for a large lattice size $L=140$. The simulation was carried out in a wide energy range (R_1 in Fig. 1) including the CrMES at the exact critical temperature (R_2 in Fig. 1). Specifically, counting the energy levels from the ground state with an integer variable $ie(=1,2,3,\ldots)$, where $ie=1$ corresponds to the ground state and the energy of a level is $E=-2N+4\cdot(ie-1)$, the simulation was carried in the wide subspace R_1: $ie=1950-3800$. The CrMES restriction applied to produce a relative accuracy ($r=10^{-6}$) on the critical specific heat (see the original paper on CrMES [45]) yields the subspace R_2: $ie=2228-3514$, while the restriction defined in Eq. (2) gives the subspace $ie=2246-3491$, which by definition determines the extent we probe the tail of the order-parameter distribution. We note that this later subspace is included in the CrMES determined from the specific heat condition (using the same level of accuracy r) and that this is a general property which does not seem to depend on the lattice size, or even on the model as far as we had the opportunity to observe. This explains the striking observation from Fig. 1 that the PDF's obtained from the subspaces R_1 and R_2 completely coincide in the x range common in both subspaces. The difference between the two curves is always smaller than the accuracy level r and, as one can observe more clearly from the inset, the part of the R_1-PDF not accessible by using the R_2 (CrMES) subspace is the range: $x=1.47-1.59$. However, the R_1-PDF appears to be already flat in this range $x=1.47-1.59$ and fitting attempts will be unstable, producing large errors. Thus the saturation range is sensibly excluded from our simulations by the CrMES restriction. The third curve, denoted as R_3 in Fig. 1 corresponds to a PDF obtained in the subspace R_3: $ie=2620-3800$, restricted severely from the saturation side. This curve is presented in order to observe that errors will be introduced if a restriction on the energy space is inappropriately applied. Noting that the errors in determining the end-points of the CrMES are of the order of 2–10 energy levels (at these lattice sizes) we conclude that critical minimum energy subspaces, with a reasonable accuracy level of the order $r=10^{-4}-10^{-6}$, will be sufficient for the study of the tail regime.

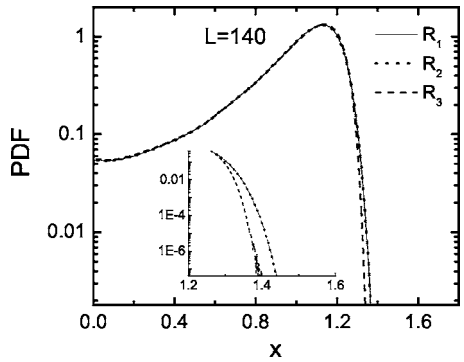

FIG. 1. Universal PDF's for a lattice of linear size $L=140$, with a logarithmic scale on the vertical axis. Three different subspaces R_1, R_2, and R_3 are used to obtain the corresponding curves. The wider subspace R_1 ($ie=1950-3800$) yields the PDF shown by the solid line. The dots demonstrate the PDF corresponding to the subspace R_2 ($ie=2228-3514$) and as can be seen from the inset the two cases coincide in their common part. R_2 is the CrMES defined by the specific heat's accuracy condition, as discussed in the text. Finally, the dashed curve, R_3 case ($ie=2620-3800$), illustrates that errors will be introduced by an inappropriate restriction of the energy space.

III. UNIVERSAL FEATURES AND THE TAIL REGIME OF THE ORDER-PARAMETER DISTRIBUTION

The universal scaling distribution of the order-parameter may be obtained from the magnetization distributions $p_m(m)$, constructed with the help of the numerical scheme outlined in the previous section, as follows [20]:

$$p(x)dx \simeq p_m(m)dm, \quad x=m/\sqrt{\langle m^2\rangle}, \quad m=M/N. \tag{4}$$

Figure 2 shows these distributions for lattice sizes $L=60$ and $L=120$. The data used were generated by the CrMES-WL (N-fold:14–24) entropic scheme using a separation refine-

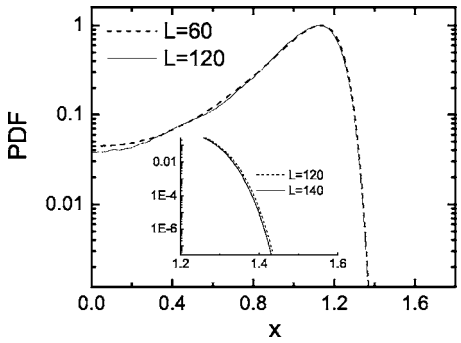

FIG. 2. Illustration of the universal scaling function $p(x)$ for $L=60$ and $L=120$. The inset is an enlargement of the right tails for the case $L=120$ and $L=140$. Note that the peak heights have been set equal to 1. In both cases a logarithmic scale on the vertical axis has been taken.

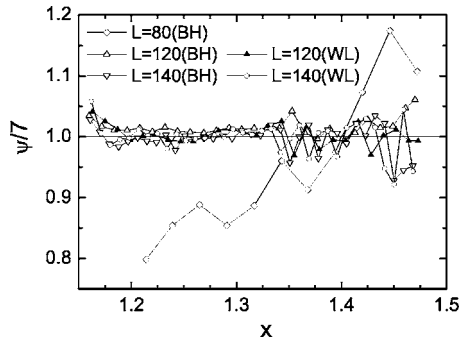

FIG. 3. Behavior of estimates of the exponent $\psi/7$ for lattice sizes $L=80$, 120, and 140, for both the WL and BH methods used. The window $x=1.2-1.3$ appears to be very stable for the sizes $L=120$ and $L=140$, where the estimates for the exponent ψ remain close to the value $\psi=7$.

ment $\mathcal{S}=16$, as explained in the previous section. The curves shown in this figure illustrate the densities obtained only via the BH approximation for the DOS and not the corresponding WL approximation of Eq. (1). This practice will be followed below in all our figures, except for the cases, indicated in the figures, where both the WL and BH DOS are used to construct and illustrate the corresponding approximations for the probability densities. Let us point out that the curves shown are lines that pass through all the points representing the sampled values of the order parameter. For a large lattice, there will be several thousands of such points, since each of them corresponds to a possible value of m $(=M/N,\ M=0,2,4,\ldots,N)$ of the finite system. The density of points on the x axis (m axis) grows with the lattice size, and we should expect to having $N/2=L^2/2$ points in the positive x axis (m axis), provided that all energies and all corresponding order-parameter values were sampled by the WL process. However, as discussed in Sec. II, the points corresponding to the saturation regime are not sampled, since this regime is excluded by the CrMES restriction applied on the energy spectrum. In order to illustrate the density functions in Fig. 2 we have chosen to identify their peak heights to the same value, set in Fig. 2 equal to unity $[\hat{p}(x^*)=1$, where x^* the most probable value]. This is equivalent to multiplying the universal PDF by a factor, which could in principle be weakly L-dependent and this dependence will be discussed further below.

Let us now consider the main conjecture for the large-x behavior of the universal function $p(x)$, [19,20]

$$p(x) \simeq p_\infty x^\psi \exp(-a_\infty x^{\delta+1}), \tag{5a}$$

with

$$\psi = \frac{\delta-1}{2} \tag{5b}$$

and p_∞, a_∞ universal constants. The structure of the exponential (5a) has been suggested by rigorous results for the two-dimensional Ising model [49] and is also consistent with Monte Carlo studies of the Ising universality class [13]. The studies of Refs. [19,20] have provided some evidence for this conjecture and in particular for the prefactor and the relation of the exponent ψ to the critical exponent δ. For the 2D Ising model the exponent should have the value $\psi=7$, if, of course, the prefactor hypothesis is valid. Smith and Bruce [20] provided numerical support for this value, but their study was not completely conclusive since it was carried out only for relatively small lattices ($L=32$ and $L=64$) and the x window in which the value $\psi=7$ was observed was actually quite narrow. We now present results for several lattice sizes ($L=80$, 100, 120, and 140) reinforcing this conjecture in a very wide x window. Following Smith and Bruce [20] we fix the exponent δ in the exponential factor of Eq. (5) and fit our results ($x>1$) in x windows, each one corresponding to 50 different magnetization values, sampled during the WL (N-fold:12–24) process. Figure 3 shows a very clear signature of the prefactor law (5b) which upholds in a large x window only for the large lattices ($L=120$ and $L=140$ are shown). On the other hand, for smaller lattice sizes $L\lesssim 80$ ($L=80$ is shown) the picture is similar to that presented in Ref. [20] and the expected value is obtained only in a small x window. In Fig. 3 we have illustrated the behavior of the estimates for the exponent ψ, and for the large lattices ($L=120$ and $L=140$) both the WL and BH cases are shown. From this figure we observe that the window $x=1.2-1.3$ is very stable for the sizes $L=120$ and $L=140$, and the estimates for the exponent ψ remain close to the value $\psi=7$, beyond small fluctuations, for even larger values of x. It appears that this stable x window may be very convenient for further fitting attempts.

Encouraged from the above finding, we now use this stable x window to perform further fitting attempts, allowing this time both exponents in the exponential and in the prefactor term vary, and use ψ as a free parameter by assuming the validity of Eq. (5b). In this way we examine whether the particular x window provides a good independent estimation of the exponent δ, based on the full tail regime conjecture [Eq. (5)]. In other words, ψ, a_∞ and p_∞ are the three free fitting parameters in applying Eq. (5) to our numerical data. Figure 4 depicts the three-parameter fitting attempts for $L=100$ and $L=120$ using both WL and BH approximations of the universal PDF. The values of the estimates for the exponent ψ and their fitting errors are illustrated in this figure. The estimates obtained for the exponent ψ are quite good in

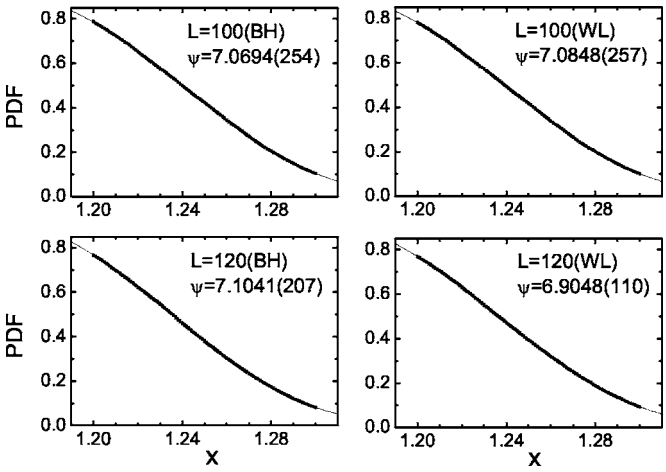

FIG. 4. Illustration of the three-parameter fitting attempts for $L=100$ and $L=120$ using both WL and BH approximations of the universal PDF. The values of the estimates for the exponent ψ and their fitting errors manifest the accuracy of our results and also the stability of the fitting attempts at the window $x=1.2-1.3$. The small differences of the exponent estimates from the two different DOS's, within the same entropic sampling runs, reflect the sensitivity of the fitting attempts to statistical errors, growing with the lattice size.

all cases and their average $\bar{\psi}=7.041$ is accurate to two significant figures, which is a rather pleasing result.

It is interesting to examine whether one could obtain reliable estimates of the universal constants a_∞ and p_∞ using the above window and to see whether such estimates can be tested against known results in the literature. It appears that the idea of such a test has not been tried in previous studies. In contrast, the main conclusion of the recent paper of Hilfer *et al.* [21] is that "the universal scaling function for the order-parameter distribution cannot be considered to be known from numerical simulations at present." Furthermore, it was stated in the conclusion of this paper that "even for the square Ising model a numerical estimation of the universal PDF requires sizes that are beyond present day computer recourses." Therefore, one would be tempted to think that, also the universal constants a_∞ and p_∞ will approach their values slowly in the asymptotic limit. Thus, a reliability test for the values of a_∞ and p_∞ estimated in the above x window will be useful even in the case where it fails. On the other hand, a test yielding a good comparison will be a strong verification of the proposal that the observed stable x window can be used for the extraction of the asymptotic behavior of the tail regime of the universal scaling function.

In order to construct a reliability test as discussed above, we shall now define following Bruce [15] the universal function $\mathcal{F}(y)$

$$\mathcal{F}(y) = \ln\left[\int dx p(x) e^{yx}\right]. \tag{6}$$

The limiting behavior of the function $\mathcal{F}(y)$ is controlled by the large-x behavior of $p(x)$ and as shown by Bruce [15] one can find, by assuming the validity of the full ansatz (5), a large y-expansion of $\mathcal{F}(y)$ which reads as

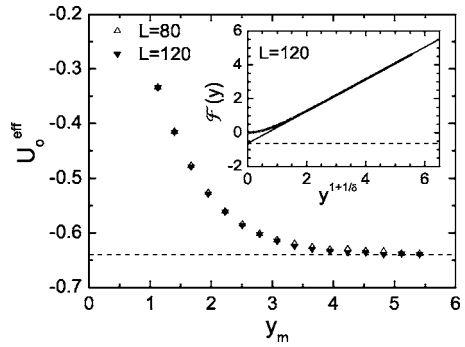

FIG. 5. Variation of U_o^{eff}, for lattices $L=80$ and $L=120$, obtained as intercepts of linear fittings of Eq. (7) in small windows in the variable $y^{1+1/\delta}$. The y_m values correspond to the center of the fitting windows. The inset shows the linear fit according to Eq. (7) in the large y part ($L=120$). The dashed line marks the exact value of the amplitude U_o for the 2D Ising model [50], approached by the corresponding intercepts. This figure should be compared to Fig. 1 of Ref. [15].

$$\mathcal{F}(y) \simeq b_\infty y^{1+1/\delta} + \frac{1}{2}\ln\left[\frac{2\pi p_\infty^2}{a_\infty \delta(\delta+1)}\right], \tag{7}$$

where b_∞ is a constant. The constant term in Eq. (7) is the universal Privman-Fisher coefficient [15]. Its value for the 2D square Ising model is $U_o=-0.639\,912$ [15,50], and as shown in Ref. [15] is related via the ansatz (5) to the universal constants a_∞ and p_∞ as follows:

$$U_o = \frac{1}{2}\ln\left[\frac{2\pi p_\infty^2}{a_\infty \delta(\delta+1)}\right]. \tag{8}$$

The expansion (7) above has been fully illustrated by Bruce [15], using appropriate y windows to observe the development of the effective U_o (U_o^{eff}) in the large y range. The agreement of this development towards the universal Privman-Fisher coefficient was shown to be excellent (see Fig. 1 in Ref. [15]).

In Fig. 5 we reproduce Fig. 1 of Ref. [15], using our numerical data for sizes $L=80$ and $L=120$. The approach to the universal value U_o is again excellent and the $L=120$ data produce a slightly faster approach, as can be seen from this figure. The estimates of U_o^{eff} in the range of $y_m \simeq 5$ deviate from the exact value by less than 0.2%. This is an explicit confirmation that a CrMES restriction is adequate for (numerical) studies of the tail regime. As pointed out by Bruce [15], the numerical estimation of U_o via the numerical integration [see Eq. (6)], illustrated above, is more reliable than attempting a direct Monte Carlo determination of free energies [15,17] or attempting to estimate U_o via the factors appearing in Eq. (8). In accordance with our earlier discussion, an accurate estimation of the universal constants a_∞ and p_∞ would not be normally expected at these lattice sizes and corrections to scaling may complicate the situation.

We proceed to describe an estimation procedure for the universal constants a_∞ and p_∞, based on the stable window $x=1.2-1.3$. As can be seen from the fitting attempts in Fig. 4, the estimates for the critical exponent ψ suffer from statistical fluctuations and are sensitive to both the DOS statis-

TABLE I. Estimates for the universal parameters and the Privman-Fisher coefficient.

Method[a]					U_o
	$\hat{p}_\infty$	$p(x^*)$	p_∞	a_∞	
WL	0.6258(240)	1.309(51)	0.8190(449)	0.0571(32)	−0.589(63)
BH	0.6172(110)	1.303(30)	0.8042(234)	0.0561(20)	−0.599(34)
	$\hat{p}_{z,\infty}$	$p_z(x^*)$	$p_{z,\infty}$	$a_{z,\infty}$	
WL	0.4476(269)	1.252(52)	0.5604(156)	0.0266(9)	−0.589(33)
BH	0.4462(132)	1.246(30)	0.5560(213)	0.0268(5)	−0.599(40)

[a]WL: $\lambda=0.951(11)$, BH: $\lambda=0.953(5)$.

tical method (WL or BH) and to the lattice size. It is therefore very important to repeat the statistical sampling and to use several lattice sizes in order to be able to observe systematic dependencies that may effect the estimated values. A fully converged implementation of the WL algorithm will be essential for the accurate application of the scheme and, of course, as usually repeated applications should improve the scheme.

Thus, we have applied a well-saturated (see the discussion in Sec. II) CRMES-WL(N-fold:16–30) entropic scheme using a separation refinement $\mathcal{S}=8$ for the N-fold levels $j=16-26$ and a separation refinement $\mathcal{S}=16$ for the N-fold levels $j=27-30$. In each run we used four such WL random walks to estimate the average WL DOS and to obtain the corresponding BH DOS. At the end of the run the cumulative $H_{\mathrm{WL}}(E,M)$ histograms were used with the above DOSs to obtain the corresponding universal PDF's. This process was repeated 4 times for each of the lattices sizes $L=90$, 100, 110, 120, and 140. For each lattice size, and each of the above runs (consisting of the 4 WL random walks) we fitted the function (5a) in the stable window $x=1.2-1.3$ by fixing the value of the exponent ψ to the expected value $\psi=7$. Thus, for each lattice size we obtained mean values and statistical errors for the following parameters: the universal constant a_∞ and $\hat{p}_\infty$, where $\hat{p}_\infty$ absorbs the identification of all peak heights to 1. The multiplying factor, thus absorbed in our notation by using $\hat{p}_\infty$, is the peak height $p(x^*)$ [$p_\infty=\hat{p}_\infty\cdot p(x^*)$]. The peak height was also estimated for each run separately as well as the parameter $\lambda=L^{-1/8}/\sqrt{\langle m^2\rangle}$ which connects the universal PDF in the scaling variable $x=m/\sqrt{\langle m^2\rangle}$ [15] with the universal PDF in the scaling variable $z=mL^{1/8}$ used by Hilfer *et al.* [19] ($z=\lambda^{-1}x$). Our fitting attempts were also repeated in this z representation using the equivalent stable window which has been taken to be $z=1.26-1.36$. For the parameters in this z representation the following notation was used: $p_{z,\infty}$ and $a_{z,\infty}$ for the universal constants controlling the tail regime, and $p_z(x^*)$ for the peak height.

Using the above described fitting attempts we observed no systematic L dependency, in the range $L=90-140$. This observation concerns all the estimated parameters, and it appears that not even weak L corrections should be applied. In fact the picture, obtained for each parameter, resembles effectively a statistical fluctuation around a mean value. Therefore it seems sensible to average the values of all parameters over the range $L=90-140$ (assuming no systematic L dependency) and take as respective errors three standard deviations of the averaging process. The values of all parameters obtained from this hypothesis are collected in Table I and are presented for the methods corresponding to the WL DOS (WL) and the BH DOS (BH). Both x and z representations were used in the fittings and the average for λ is also given in the footnote of Table I. Using these values in conjunction with Eq. (8) and the exact value for the state exponent $\delta=15$ [note also that $p_\infty=\hat{p}_\infty\cdot p(x^*)$], the respective estimate for the universal Privman-Fisher coefficient is determined for each case and is presented in Table I.

Discussing Table I we first observe that all parameters involved in the estimation of the universal Privman-Fisher coefficient have reasonable relative errors of the order of 2%–4%. The corresponding relative errors for U_o are of the order of 4%–10%. However, the values obtained for U_o are lower than the exact value and the underestimation is of the order of 7%. This, compared to the excellent agreement obtained by the numerical integration method shown in Fig. 5 and discussed above reveals the superiority of the integration method. The origin of the present underestimation is not clear. One may think that, moving to a x window corresponding to larger values of x could improve the above picture. Nevertheless, we have checked that this is not so, and that statistical errors become dominant as we move to larger x values, making the estimation scheme unreliable. Finally, let us compare the constant $a_{z,\infty}=0.026\ldots$ of Table I with the coefficient of the exponential term given in Eq. 7 of Ref. [19]. This latter coefficient has the value $\frac{1}{\delta}\left(\frac{\delta}{\delta+1}\right)^{\delta+1}=0.023738\ldots$ for the square Ising model. These two values are of the same order, although corresponding to different scaling limits [19], and this is an indication in favor of the reliability of the stable x window discussed here. It also strongly supports the proposal of Hilfer and Wilding [19] to calculate critical finite-size scaling functions via the generalized classification theory of phase transitions developed by Hilfer [29–32]. It will be interesting to uncover the reasons behind the minor underestimation of the universal Privman-Fisher coefficient by the direct estimation of the universal constants a_∞ and p_∞, as attempted in this work.

Finally, we briefly discuss the behavior of the left tails of the critical distributions. This behavior has been considered by Hilfer *et al.* [21] by using rescaled probability densities $p_o(x)$, where x and p_o are defined in such a way that yield mean zero, unit norm, and unit variance [21]. This new scaled variable x should not be confused with the scaled variable x defined in Eq. (4) and appearing in Figs. 1–4.

These new distributions are appropriately translated with respect to the position of the peak of the distribution (x_{peak}) for each tail separately. For instance for the left tail one defines: $p_{ol}(x)=p_o(x_{\text{peak}}-x)$ with $x<x_{\text{peak}}$. Furthermore, these authors used plots of the functions $q(y)=\frac{d\log(-\log p_{ol})}{d\log x}$ versus $y=\log x$, and compared their tail behavior with the standard Gaussian behavior. The large x range of these plots is convenient for illustrating the possible developments of fat stretched exponential tails of the form $\sim\exp[-x^{\omega}]$. Using their method we have also tried to clarify the behavior of the left tails of our critical distributions for all sizes up to $L=140$. Qualitatively, we found the same behavior with that of Ref. [21]. In particular a data collapse for all sizes up to $L=140$ was observed and the picture is very similar with their behavior (see the right upper row of Fig. 6 in Ref. [21]). However, it should be noted that, the data corresponding to the left tails suffer from relatively stronger fluctuations when compared with the data of the right tails. This is due to the inevitable more limited magnetic sampling in the left tails. Note that, the left tails are strongly influenced from a part of the energy spectrum in which a much larger number of spin configurations exists, compared with the lower energy part of the spectrum determining the right tails. However, using relatively larger x windows (corresponding to at least 250 different magnetization values for $L=120$) we have tried to repeat the small x windows fitting attempts, as those shown in our Fig. 3. In this case we used as a test function the simple exponential behavior $p_{ol}(x)=q\exp[-bx^{\omega}]$, and the total fitting range of the new scaled variable x was $x=1-3.25$, which we assume describes the left tail regime. Note that this range corresponds to the range $x=0.87-0.28$ of our Fig. 2 for the scaled variable defined in Eq. (4). For the lattice $L=120$ the total fitting range includes about 2400 different magnetization values. Remarkably, we have obtained almost the same behavior for $L=50$ and $L=120$. For both sizes we found that for the above rather large range (1–3.25) the exponent ω steadily decreases (almost linearly for $L=120$) from the value $\omega=0.75$ to the value 0.15 passing through the value $\omega=0.5$ in the neighborhood of $x=1.75$. For larger values of x outside the above range (1–3.25) the statistical fluctuations do not permit reasonable fits. The described behavior is consistent with that of Ref. [21] and since it is observed for the small and the larger lattice sizes we may suppose that it represents also the true asymptotic behavior. As a final remark we point out that the fat stretched exponential left tail $\sim\exp[-\sqrt{x}]$ reported in Ref. [21] at the low temperature $T=1.5$ can not be studied by our data. Such a study would require the application of the present scheme in a lower part of the energy space.

IV. CONCLUSIONS

In the present Monte Carlo study we applied the CrMES-WL entropic sampling scheme, based on the high-levels of the Wang-Landau process in dominant energy subspaces, in order to obtain the order-parameter universal PDF of the square Ising model for large lattices. The efficiency of this method enabled us to clarify the asymptotic tail behavior of the universal distribution and to obtain reliable data for the universal parameters. In particular, we found that there exists a large stable window of the scaled order parameter in which the full ansatz for the tail regime is well obeyed. In a second stage, this window was used to estimate the equation of state exponent δ and also to observe the behavior of the universal constants implicit in the functional form of the universal PDF and to approximate for the first time their values. The estimates of the universal constants appear to be reliable to within 3%–7% of statistical errors. The excellent accuracy obtained for the universal Privman-Fisher coefficient, by appropriate numerical integration, was also illustrated and consists a concrete reliability test of the accuracy of our numerical scheme.

ACKNOWLEDGMENTS

This research was supported by EPEAEK/PYTHAGORAS under Grant No. 70/3/7357. One of us (N.G.F.) would like to thank the Empeirikeion Foundation for financial support.

[1] J. Cardy, *Scaling and Renormalization in Statistical Physics* (University Press, Cambridge, 1996).
[2] M. E. Fisher, Rep. Prog. Phys. **30**, 615 (1967).
[3] R. J. Baxter, *Exactly Solved Models in Statistical Mechanics* (Academic, London, 1982).
[4] H. E. Stanley, *Introduction to Phase Transitions and Critical Phenomena* (Oxford University Press, Oxford, 1971).
[5] N. Goldenfeld, *Lectures on Phase Transitions and the Renormalization Group* (Addison-Wesley, Reading, 1992).
[6] L. P. Kadanoff, *Scaling at Critical Points*, edited by C. Domb and M. S. Green (Academic, London, 1976).
[7] V. Privman, in *Finite-Size Scaling and Numerical Simulation of Statistical Systems*, edited by V. Privman (World Scientific, Singapore, 1990).
[8] M. E. Fisher, in *Critical Phenomena, Proceedings of the International School of Physics*, "Enrico Fermi," 1970, edited by M. S. Green (Academic, New York, 1971).
[9] M. N. Barber, *Phase Transitions and Critical Phenomena*, edited by C. Domb and J. L. Lebowitz (Academic, New York, 1983).
[10] V. Privman and M. E. Fisher, Phys. Rev. B **30**, 322 (1984).
[11] A. D. Bruce, J. Phys. A **18**, 873 (1985).
[12] K. Binder, Z. Phys. B: Condens. Matter **43**, 119 (1981).
[13] D. Nicolaides and A. D. Bruce, J. Phys. A **21**, 233 (1988).
[14] A. Z. Patashinskii, Sov. Phys. JETP **26**, 1126 (1968).
[15] A. D. Bruce, J. Phys. A **28**, 3345 (1995).
[16] A. D. Bruce, T. Schneider, and E. Stoll, Phys. Rev. Lett. **43**, 1284 (1979).
[17] K. K. Mon, Phys. Rev. Lett. **54**, 2671 (1985).
[18] A. D. Bruce and N. B. Wilding, Phys. Rev. Lett. **68**, 193 (1992).
[19] R. Hilfer and N. B. Wilding, J. Phys. A **28**, L281 (1995).

[20] G. Smith and A. Bruce, J. Phys. A **28**, 6623 (1995).
[21] R. Hilfer, B. Biswal, H. G. Mattutis, and W. Janke, Phys. Rev. E **68**, 046123 (2003).
[22] R. Botet and M. Ploszajczak, Phys. Rev. E **62**, 1825 (2000).
[23] E. Eisenriegler and R. Tomaschitz, Phys. Rev. B **35**, 4876 (1987).
[24] J. Cardy, in *Finite-Size Scaling*, edited by J. Cardy (North-Holland, Amsterdam, 1988).
[25] X. Chen, V. Dohm, and A. Talapov, Physica A **232**, 375 (1996).
[26] A. Bruce, J. Phys. C **14**, 3667 (1981).
[27] E. Brezin and J. Zinn-Justin, Nucl. Phys. B **257**, 867 (1985).
[28] T. W. Burkhardt and B. Derrida, Phys. Rev. B **32**, 7273 (1985).
[29] R. Hilfer, Phys. Scr. **44**, 321 (1991).
[30] R. Hilfer, Phys. Rev. Lett. **68**, 190 (1992); Mod. Phys. Lett. B **6**, 773 (1992).
[31] R. Hilfer, Int. J. Mod. Phys. B **7**, 4371 (1993); Phys. Rev. E **48**, 2466 (1993).
[32] R. Hilfer, Z. Phys. B: Condens. Matter **96**, 63 (1994).
[33] N. Metropolis, A. W. Rosenbluth, M. N. Rosenbluth, A. H. Teller, and E. Teller, J. Chem. Phys. **21**, 1087 (1953).
[34] A. B. Bortz, M. H. Kalos, and J. L. Lebowitz, J. Comput. Phys. **17**, 10 (1975).
[35] K. Binder, Rep. Prog. Phys. **60**, 487 (1997).
[36] M. E. J. Newman and G. T. Barkema, *Monte Carlo Methods in Statistical Physics* (Clarendon, Oxford, 1999).
[37] D. P. Landau and K. Binder, *A Guide to Monte Carlo Simulations in Statistical Physics* (Cambridge University Press, Cambridge, 2000).
[38] M. M. Tsypin and H. W. J. Blöte, Phys. Rev. E **62**, 73 (2000).
[39] J. Lee, Phys. Rev. Lett. **71**, 211 (1993).
[40] B. A. Berg and T. Neuhaus, Phys. Rev. Lett. **68**, 9 (1992).
[41] P. M. C. de Oliveira, T. J. P. Penna, and H. J. Hermann, Braz. J. Phys. **26**, 677 (1996); P. M. C. de Oliveira, *ibid.* **30**, 195 (2000).
[42] J.-S. Wang and R. H. Swendsen, J. Stat. Phys. **106**, 245 (2002); J.-S. Wang, T. K. Tay, and R. H. Swendsen, Phys. Rev. Lett. **82**, 476 (1999).
[43] F. Wang and D. P. Landau, Phys. Rev. Lett. **86**, 2050 (2001); Phys. Rev. E **64**, 056101 (2001); B. J. Schulz, K. Binder, M. Muller, and D. P. Landau, *ibid.* **67**, 067102 (2003).
[44] A. Malakis, S. S. Martinos, I. A. Hadjiagapiou, N. G. Fytas, and P. Kalozoumis, Phys. Rev. E **72**, 066120 (2005).
[45] A. Malakis, A. Peratzakis, and N. G. Fytas, Phys. Rev. E **70**, 066128 (2004).
[46] S. S. Martinos, A. Malakis, and I. A. Hadjiagapiou, Physica A **352**, 447 (2005).
[47] B. J. Schulz, K. Binder, and M. Muller, Int. J. Mod. Phys. C **13**, 477 (2002).
[48] A. Malakis, S. S. Martinos, I. A. Hadjiagapiou, and A. S. Peratzakis, Int. J. Mod. Phys. C **15**, 729 (2004).
[49] B. McCoy and T. Wu, *The Two-Dimensional Ising Model* (Harvard University Press, Cambridge, 1972).
[50] A. E. Ferdinand and M. E. Fisher, Phys. Rev. **185**, 832 (1969).
[51] P. Dayal, S. Trebst, S. Wessel, D. Würtz, M. Troyer, S. Sabhapandit, and S. N. Coppersmith, Phys. Rev. Lett. **92**, 097201 (2004).
[52] C. Zhou and R. N. Bhatt, Phys. Rev. E **72**, 025701(R) (2005).
[53] H. K. Lee, Y. Okabe, and D. P. Landau, cond-mat/0506555.
[54] D. Brudy and B. Meister, Phys. Rev. Lett. **76**, 1 (1996).